

Interaction between Zeolites and Cluster Compounds

Part 1.—Adsorption of Iron Pentacarbonyl on Zeolites

BY THOMAS BEIN† AND PETER A. JACOBS*

Centrum voor Oppervlaktescheikunde en Colloïdale Scheikunde, Katholieke Universiteit Leuven, de Croylaan 42, B-3030 Leuven (Heverlee), Belgium

Received 11th November, 1982

The adsorption isotherms of $\text{Fe}(\text{CO})_5$ on NaY, HY and Linde L zeolites obtained in McBain balances show micropore adsorption, whereas additional capillary condensation is found with zeolite omega and Na-mordenite. The pores and/or cages of the zeolites studied are completely filled with the complex upon saturation, with the exception of Na-mordenite. Their behaviour is explained, respectively, by pore blocking and the occurrence of channel openings that are too narrow. The silicalite channel system also is too narrow to accept $\text{Fe}(\text{CO})_5$ molecules.

Infrared results show that an increasing interaction of the complex with faujasites exists in the sequence: dealuminated Y < CsY < HY < NaY. This is derived from the increasing band half-width of the adsorbed complex in the CO stretching region and from the increasing intensity of the ν_1 vibration, which upon adsorption becomes i.r. active. The interaction is assumed to be influenced mainly by electrostatic fields in the cages or pores, which can lead to a very restricted mobility for the encaged complex. The complex seems to remain intact upon adsorption at 293 K in all the zeolites studied.

In catalytic research on supported-metal catalysts the relationship between metal particle size and activity or selectivity of the catalyst is still not entirely understood as a result of the broad metal particle size distribution which is present in most systems. The purpose of this study was to develop preparation techniques for iron model catalysts with narrow, variable particle size distributions. Zeolites were chosen as a support for the iron phase since they possess uniform but variable pore and cage geometries and dimensions.

Iron(II)-exchanged zeolites cannot be reduced by molecular hydrogen,¹ whereas with sodium vapour as reduction agent a highly, but not uniformly, dispersed iron metal phase was obtained.^{2–4} However, both methods of preparation of iron metal zeolites have serious drawbacks. By conventional ion-exchange procedures it is difficult to prepare the materials in a reproducible way, while with sodium vapour reduction there is always the risk that the iron phase may be contaminated by Na or NaOH. Therefore the adsorption and subsequent decomposition of iron pentacarbonyl was chosen as an alternative method of preparation.

A great amount of work has been done on the anchoring and decomposition of metal carbonyls on various supports for catalyst preparations.⁵ Iron pentacarbonyl has been used to prepare iron particles on ZnO and NiO,⁶ on $\gamma\text{-Al}_2\text{O}_3$,^{7,8} on MgO ⁹ and on graphite.¹⁰

Recently, the adsorption and subsequent thermal decomposition of $\text{Fe}(\text{CO})_5$ on HY zeolites has been reported.^{11,12} From data obtained from infrared spectroscopy and

† On leave from: Institut für Physikalische Chemie der Universität Hamburg, Laufgraben 24, D-2000 Hamburg 13, Federal Republic of Germany

desorption studies the authors conclude that the initial $\text{Fe}(\text{CO})_5/\text{HY}$ adduct undergoes substitution of one CO by one lattice oxygen atom. These species are then considered to migrate in the matrix to form polynuclear iron carbonyl complexes.

A comparison of the thermal and photochemical decomposition of $\text{Fe}(\text{CO})_5/\text{HY}$ by ^{13}C -n.m.r. has also been reported.^{13, 14} The interaction of the complex and its thermal-decomposition intermediates with the matrix was found to be much smaller than that of the photochemically produced intermediates.

In the former studies only a few quantitative details are given with regard to the adsorption of the complex. Since it is a prerequisite for the reproducible preparation of these materials to obtain data on the adsorption equilibrium and on the nature of the interaction between matrix and complex, this information is reported in the present study.

The adsorption process was followed using gravimetric techniques. Since the i.r. spectrum of iron pentacarbonyl appears to be influenced by its aggregation state and by the nature of the surrounding matrix,^{15, 16} infrared spectroscopy was also selected to investigate the interactions of the complex with the zeolite matrix.

EXPERIMENTAL

MATERIALS

All zeolites used were of synthetic origin. The unit-cell composition of the dry zeolites (after degassing *in situ* for 12 h at 10^{-3} N m⁻² and 720 K) was determined by atomic absorption spectrometry and is given in table 1. A mnemonic code was used to identify the structure type.¹⁷

Table 1. Unit-cell composition of the zeolites used in this study

zeolite	chemical composition
FAU	$\text{Na}_{55.5}\text{Al}_{55.5}\text{Si}_{136.5}\text{O}_{384}$
Cs-FAU	$\text{Cs}_{37}\text{Na}_{18.5}\text{Al}_{55.5}\text{Si}_{136.5}\text{O}_{384}$
H-FAU	$\text{H}_{50}\text{Na}_{5.5}\text{Al}_{55.5}\text{Si}_{136.5}\text{O}_{384}$
FAU*	$\text{Si}_{192}\text{O}_{384}$
LTL	$\text{K}_{8.8}\text{Al}_{8.8}\text{Si}_{27.2}\text{O}_{72}$
MAZ	$\text{Na}_{6.6}\text{Al}_{6.6}\text{Si}_{29.4}\text{O}_{72}$
MOR	$\text{Na}_8\text{Al}_8\text{Si}_{40}\text{O}_{96}$
SIL	$\text{Si}_{96}\text{O}_{192}$

NaY from Strem Chemicals (FAU) and TMA-omega from Linde (Union Carbide) (MAZ) were treated with 0.1 mol dm⁻³ NaCl solution to remove possible cation deficiencies, washed until free of chloride and then air-dried. CsY (Cs-FAU) was prepared by ion exchange of NaY with 0.1 mol dm⁻³ CsCl solution at 293 K, washed and then dried.

The hydrogen-Y zeolite (H-FAU) was obtained by slow heating (a temperature rise of 2 K min⁻¹) to 720 K *in vacuo* (10^{-3} N m⁻²) of the NH_4 -form. The latter sample was prepared from NaY by ion exchange with a solution of 0.1 mol dm⁻³ NH_4Cl .

Dealuminated Y (FAU*) was prepared from NH_4Y as follows. The exchanged form was washed, dried and calcinated in water vapour at 820 K to give the ultrastable form.¹⁸ The dried product was subsequently treated with SiCl_4 vapour in a helium stream at 820 K for 24 h to extract the aluminium.¹⁹ In order to obtain a hydrogen-free product, the zeolite was calcined at 1220 K for 20 h.

Silicalite (SIL) was made by synthesis, using aerosil, NaOH and a tetrapropylammonium hydroxide solution as reactants, in a similar manner to that reported for the synthesis of ZSM-5.²⁰ Linde L (LTL) and Na-mordenite (MOR) from Norton were used without pretreatment.

Before use, all zeolites were stored over saturated NH_4Cl solution in order to ensure constant humidity.

Iron pentacarbonyl from Ventron (99.5%) was cold-distilled in the dark and stored over molecular sieve 5A. The zeolite samples were loaded in the McBain balance or in the i.r. cell as follows. The carbonyl was frozen in liquid air, outgassed in a vacuum and allowed to warm up until the desired pressure was reached. Light was carefully excluded throughout the measurements in order to avoid photodecomposition of the iron pentacarbonyl. The weight measurements in the McBain balance were carried out in weak red light.

METHODS

The adsorption isotherms were obtained at 293 K in an all-glass McBain balance, using greaseless valves and a calibrated quartz spring with a precision of $\pm 0.5\%$. The pressure was recorded with a Bell & Howell pressure transducer (BHL-4100-01), which is linear within $\pm 0.5\%$ up to 75 kN m^{-2} . After each admission of gas an equilibration time of 1 h was allowed, since preliminary experiments showed that no further uptake occurred during the next 3 h.

The infrared spectra were recorded with a Perkin-Elmer 580 B spectrometer in the $4000\text{--}1200 \text{ cm}^{-1}$ range. For frequency measurements a scan mode was used with resolution better than 1.5 cm^{-1} . The zeolite was pressed at 0.1 GN m^{-2} into self-supporting wafers of *ca.* 5 mg cm^{-2} and introduced into a quartz cell of 80 mm path length and equipped with CaF_2 windows of 3 mm thickness. The cell could be heated and was connected to a greaseless gas-dosing and handling system.

Gravimetric measurements were carried out in a thermobalance (Mettler Thermoanalyser 2) under a purge of dry helium in the 10 and 1 mg range. Samples of $10 \pm 2 \text{ mg}$ of zeolite were loaded with $\text{Fe}(\text{CO})_5$ at 293 K in a stream of dry helium ($2.8 \text{ dm}^3 \text{ h}^{-1}$) containing *ca.* 0.4 kN m^{-2} of adsorbent.

RESULTS AND DISCUSSION

ADSORPTION ISOTHERMS OF $\text{Fe}(\text{CO})_5$ ON ZEOLITES FAU, H-FAU, LTL, MAZ, MOR AND SIL

The adsorption isotherms of $\text{Fe}(\text{CO})_5$ on zeolites as obtained in the McBain balance at 293 K are plotted in fig. 1 and 2. According to their form, the isotherms can be classified into two groups. Adsorption on zeolites Y and L shows a typical micropore-filling behaviour since the major uptake occurs at very low relative pressures.²¹ Almost 80% saturation loading is already reached at $p/p_0 = 0.01$, whereas complete saturation is observed for $p/p_0 > 0.1$. At a relative pressure of 0.5, H-FAU, FAU and LTL adsorb 42, 39 and 12.5 mg of $\text{Fe}(\text{CO})_5$ per 100 mg dry zeolite, respectively. Only a small amount of capillary condensation, starting at relative pressures of *ca.* 0.9, is observed.

Different adsorption behaviour is found for zeolites MAZ, MOR and SIL. With MAZ and MOR there is no discrete saturation region. Adsorption proceeds *via* a sigmoid-type uptake curve, and capillary condensation starts at low relative pressures.

At a relative pressure of 0.5, MAZ, MOR and SIL adsorb 20, 3.5 and 0.5 mg $\text{Fe}(\text{CO})_5$ per 100 mg dry zeolite, respectively. Since the adsorption is fully reversible down to small relative pressures, even in the case of MAZ, capillary condensation must be due to materials with a large outer surface area (*i.e.* particle size $< 10 \text{ nm}$) and/or mesopores in the nanometre range, presumably caused by the calcination treatment. Since the actual size of the MAZ crystals is in the $1\text{--}3 \mu\text{m}$ range, the second possibility is preferred, although an explanation for mesopore formation cannot be advanced.

The adsorption behaviour of SIL indicates that the iron pentacarbonyl is unable to enter the pores. The uptake is easily explained by monolayer adsorption on the external surface of the crystallites. Assuming an effective radius of 0.35 nm for the carbonyl molecule, 0.3% by weight is adsorbed *via* this process on $1 \mu\text{m}$ sized crystallites.

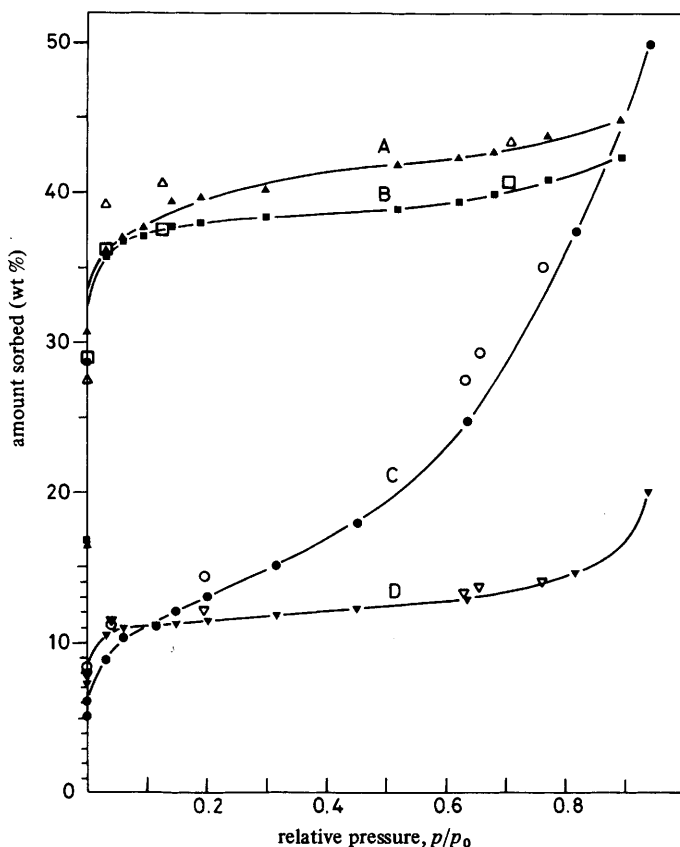


Fig. 1. Adsorption isotherms of $\text{Fe}(\text{CO})_5$ on (A) H-FAU, (B) FAU, (C) MAZ and (D) LTL at 293 K ($p_0 = 2.94 \text{ kN m}^{-2}$); full symbols, adsorption; open symbols, desorption.

DEGREE OF PORE OR CAGE FILLING WITH IRON PENTACARBONYL AT SATURATION CONDITIONS

The quantities of iron pentacarbonyl adsorbed are now discussed in terms of the degree of filling of the cages or pores. The amounts adsorbed on the zeolites at saturation (293 K, $p = 0.4 \text{ kN m}^{-2}$ and $p/p_0 = 0.136$) are listed in table 2 and are compared with data obtained thermoanalytically. The partial pressure used (0.4 kN m^{-2}) is suitable for a comparison of the loadings on the various different zeolite samples since the isotherms indicate that at this pressure the saturation state has been reached and capillary condensation is still absent.

The faujasite structure clearly shows the highest sorption capacity, corresponding on average to three molecules per supercage. Geometrically it is perfectly possible to accommodate 3 spheres with an effective radius of 0.35 nm into the faujasite supercage of 1.3 nm diameter. It should be stressed that this way the cages are completely filled since the sorption capacity seems to decrease when larger charge-compensating cations are present in these cages (see Cs-FAU).

The one-dimensional channel structures LTL and MAZ take up *ca.* 1.5 molecules of $\text{Fe}(\text{CO})_5$ per unit cell or per channel. Given the cage dimensions for LTL and MAZ (table 2) and their deviations from pure cylindrical geometry due to the existence of

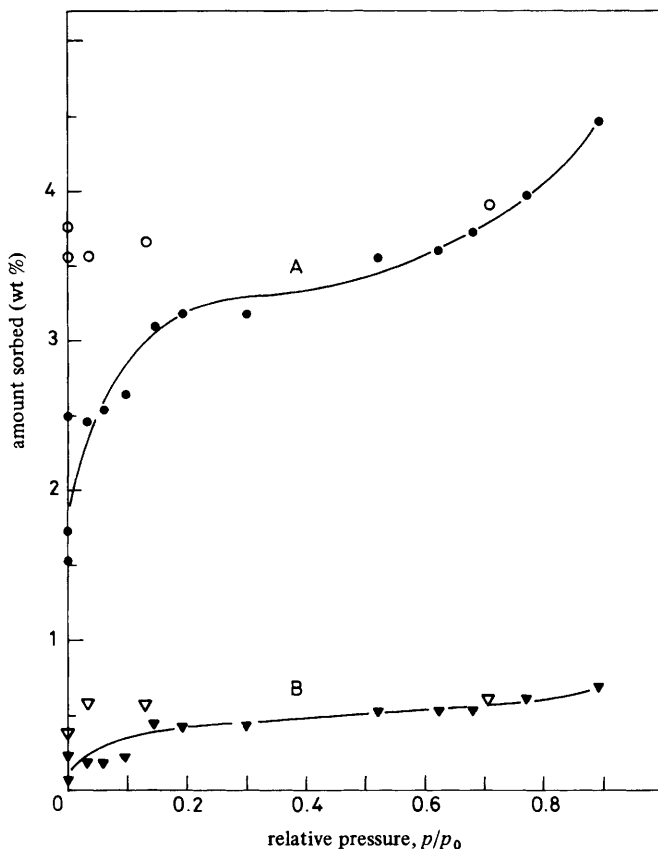


Fig. 2. Adsorption isotherms of $\text{Fe}(\text{CO})_5$ on (A) MOR and (B) SIL at 293 K ($p_0 = 2.94 \text{ kN m}^{-2}$); full symbols, adsorption; open symbols, desorption.

Table 2. Saturation loadings of $\text{Fe}(\text{CO})_5$ adsorbed on zeolites at 293 K and $p/p_0 = 0.136$ ($p = 0.4 \text{ kN m}^{-2}$)

zeolite	weight % from		molecules		pore/cage fraction filled ^a	pore/cage dimensions ^b /nm
	McBain balance	thermo-balance	per unit cell	per cage		
FAU	37.8	38.3	24.7	3.1 ^c	0.48	1.3
Cs-FAU	—	24.6	21.1	2.6 ^c	0.41	1.3
H-FAU	39.3	38.9	23.3	2.9 ^c	0.46	1.3
LTL	11.3	11.7	1.47	1.5 ^d	0.89	0.71 × 0.75
MAZ	11.8	9.4	1.3	1.3 ^d	0.72	0.74 × 0.76
MOR	3.0	3.4	0.50	0.25 ^e	0.16	0.67 × 0.70 × 0.75
SIL	0.4	—	0.1	0.05 ^e	0.02	0.54 × 0.56 × 1.99

^a Volume of $\text{Fe}(\text{CO})_5$ adsorbed (assuming a radius of 0.35 nm) divided by the channel volume per unit cell; ^b according to ref. (17); ^c per supercage; ^d per unit cell (1 channel); ^e per channel (2 per unit cell).

'side pockets', it follows that the pores have to be filled completely under these conditions of temperature and relative pressure.

For molecules which cannot diffuse through eight-membered rings of oxygen atoms, MOR shows a one-dimensional channel system. Only 0.50 molecules of $\text{Fe}(\text{CO})_5$ per unit cell or 0.25 molecules per channel are adsorbed in this structure, six times less than with LTL or MAZ. This amount of sorbate is too high to be explained by monolayer adsorption at the external surface, and therefore pore-mouth blocking must have occurred. Unfortunately this cannot be tested by using elevated sorption temperatures since the sorbate would start to decompose.²² Intuitively, this mechanism of pore-mouth blocking is understandable since the pore size of MOR is elliptical (table 2) and very close to the effective diameter of iron pentacarbonyl.

The silicalite structure seems to be inaccessible to iron pentacarbonyl penetration: only 0.05 molecules per cage are adsorbed. The amount adsorbed can easily be explained by monolayer adsorption on the zeolite crystals, as discussed above.

For all samples the fraction of the total channel volume occupied by the $\text{Fe}(\text{CO})_5$ molecules was calculated (table 2), using a sphere of radius 0.35 nm as the sorbate. The most favourable packing is observed for the structures with one-dimensional pores (LTL and MAZ). However, as a result of their higher specific pore volume, the faujasites adsorb by far the greatest amount of carbonyl.

Table 3. Irreversibly sorbed $\text{Fe}(\text{CO})_5$ after degassing the zeolites for 15 h at 10^{-3} N m⁻² and 293 K

zeolite	weight %	molecules per cage
FAU	28.3	2.3 ^a
H-FAU	27.1	2.0 ^a
LTL	7.67	1.0 ^b
MAZ	7.98	0.9 ^b
MOR	3.6	0.3 ^c
SIL	0.4	0.05 ^c

^a Per supercage; ^b per unit cell (1 channel); ^c per channel (2 per unit cell).

IRREVERSIBLY SORBED IRON PENTACARBONYL

The $\text{Fe}(\text{CO})_5$ -loaded zeolites were subjected to a degassing treatment at 293 K for 15 h using a dynamic vacuum of 10^{-3} N m⁻². The amounts of the sorbed complex remaining are listed in table 3. The adsorption process in no case is completely reversible. At least 70% of the loading at $p/p_0 = 0.136$ is left in the zeolite after a thorough room-temperature degassing.

In situ infrared desorption experiments in comparable conditions also show only a 10% decrease in overall band intensity in the CO-stretching region. These results show that a strong adsorption of the iron pentacarbonyl molecule occurs in zeolites. The i.r. results given below indicate that the sorbate molecules remain chemically stable in the zeolite pores or cages.

ADSORPTION FREQUENCIES OF $\text{Fe}(\text{CO})_5$ IN THE ZEOLITE ADDUCT

Information about the adsorption state of $\text{Fe}(\text{CO})_5$ can be obtained from the stretching vibrations of CO. The i.r. and Raman frequencies of $\text{Fe}(\text{CO})_5$ between 2140 and 1930 cm⁻¹ in the gaseous, liquid and solid states and their proposed assignments are summarized in table 4. Good experimental agreement (within ± 1 cm⁻¹) is

Table 4. Assignments of the i.r. frequencies of Fe(CO)₅ between 2140 and 1930 cm^{-1a}.

i.r., gaseous ^b		i.r., liquid		Raman, liquid, ref. (24)	Raman, solid, ref. (24)	i.r., solid, ref. (15)
ref. (23)	ref. (28)	ref. (23)	ref. (24)	ref. (15) ^c		
2124 w (ν ₁₀ + ν ₁₄)	2142 (ν ₂ + ν ₆) (ν ₂ + ν ₁₄)	2148 w (ν ₁₀ + ν ₁₄)				
2127 w (ν ₁₀ + ν ₁₈)	2127 (ν ₆ + ν ₁₈)	2118 w (ν ₁₀ + ν ₁₈)		2108	2117 (ν ₁)	2115 (ν ₁) ^d
2110 m (ν ₆ + ν ₁₈)	2109 (ν ₁₀ + ν ₁₈)	2110 m (ν ₆ + ν ₁₈)		2091		
2087 m (ν ₂ + ν ₁₄)	2087 (ν ₁₀ + ν ₁₅)	2088 m (ν ₂ + ν ₁₄)		2038	2030 vs (ν ₂)	2033 (ν ₂)
2034 vvs (ν ₆)	2034 (ν ₆)	broad band		2016	2022 (ν ₂)	2017 sh
2014 vvs (ν ₁₀)	2013 (ν ₁₀)		2002 (ν ₆)	1984	1999/71 (ν ₁₀)	2003 (ν ₆)
1976 vs [ν(¹³ C)]	1976 (¹³ C)		1979 (ν ₁₀)	1960		1982/77 (ν ₁₀)
1935 (ν ₁₀ - ν ₁₈) (ν ₁₀ - ν ₁₄)	1939 (ν ₁₀ - ν ₁₅)	1935 m (ν ₁₀ - ν ₁₈) (ν ₁₀ - ν ₁₄)				1956/48 (¹³ C)

^a w = weak, m = medium, s = strong, vvs = very strong, vs = very strong, vvs = very strong absorbance; ^b shoulders not assigned are excluded; ^c no assignment given; ^d the ν₁ vibration becomes i.r. active when the local symmetry is changed from D_{3h} to C_{3v} or to C_{2v}.

obtained for the vibrations in the gaseous state between two literature sources and the gas-phase spectra of the present work. The published spectra for the liquid state show differences in frequency and in the number of bands. A general observation is that the gas-phase spectrum is considerably broadened on going from the gaseous to the liquid state. Also disagreement exists as to the assignment of the combination vibrations, which represent the weaker bands.

In the wavenumber range reported only the assignment of bands at 2034, 2014 and 1976 cm^{-1} to the ν_6 , ν_{10} and $\nu(^{13}\text{C})$ vibration mode, respectively, seems to be unambiguous. The notation used is the one proposed by Edgell *et al.*²³

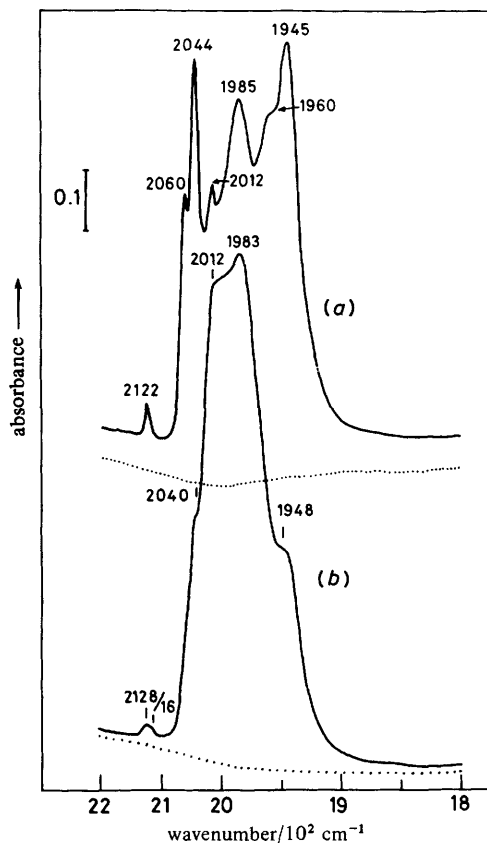


Fig. 3. Infrared spectra of $\text{Fe}(\text{CO})_5$ /zeolite adducts in the CO stretching region at 293 K (saturated for 10%): (a) $\text{Fe}(\text{CO})_5$ /FAU; (b) $\text{Fe}(\text{CO})_5$ /Cs-FAU; dotted lines, zeolite wafers degassed at 720 K for 2 h prior to adsorption.

The Raman spectrum of liquid $\text{Fe}(\text{CO})_5$ shows bands at 2116 (ν_1), 2030 (ν_2) and 1889 (ν_{10}) cm^{-1} of medium (m), very strong (vs) and strong (s) intensity, respectively. The vibration at 2116 cm^{-1} was assigned to the i.r.-inactive totally symmetric ν_1 mode.²⁴ Compared to the liquid state, the Raman vibrations of $\text{Fe}(\text{CO})_5$ in the solid state shift only slightly in frequency and the ν_{10} mode is split into components at 1999 and 1971 cm^{-1} .²⁴

In the i.r. spectrum of solid $\text{Fe}(\text{CO})_5$ ¹⁵ the Raman inactive ν_6 mode at 2003 cm^{-1} as well as the totally symmetric ν_1 mode (at 2115 cm^{-1}) become active. This is the result

of a decrease in the site symmetry of $\text{Fe}(\text{CO})_5$ to C_2 in the crystalline state, which leads to i.r. activation of all molecular vibrations.¹⁵ A change in the local symmetry from D_{3h} to C_{3v} ²⁴ is also expected to activate the ν_1 mode in the i.r. This can be achieved by substitution of the axial ligands of the complex.²⁴ In conclusion, the appearance of the ν_1 vibration can give an indication of the degree of perturbation of the local symmetry and of the extent to which the perturbed molecules interact with their environment.

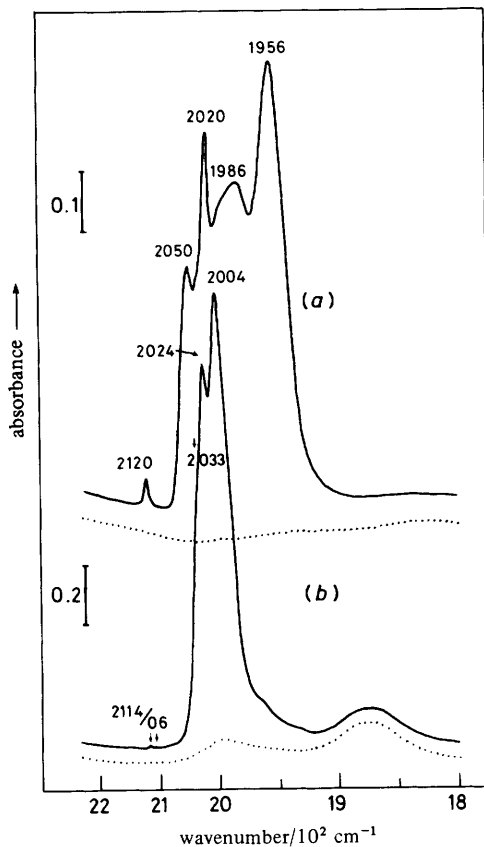


Fig. 4. Infrared spectra of $\text{Fe}(\text{CO})_5$ /zeolite adducts in the CO stretching region at 293 K (saturated for 10%): (a) $\text{Fe}(\text{CO})_5$ /H-FAU; (b) $\text{Fe}(\text{CO})_5$ /FAU*; dotted lines, zeolite wafers degassed at 720 K for 2 h prior to adsorption.

In the present study, $\text{Fe}(\text{CO})_5$ vapour at a partial pressure of 3.0 N m^{-2} was contacted for *ca.* 10 s with wafers of FAU, Cs-FAU, H-FAU, FAU* and LTL at 293 K. The amount of $\text{Fe}(\text{CO})_5$ adsorbed corresponds then to *ca.* 10% of the saturation value. Only with MAZ and MOR did the wafers show sufficient transmission to permit scans at total saturation. These spectra were obtained by contacting the wafers with 0.88 kN m^{-2} of $\text{Fe}(\text{CO})_5$ vapour for 1 h.

Fig. 3–5 show the infrared pattern obtained in the CO stretching region after sorption of iron pentacarbonyl. The spectra of the respective samples are distinctly different. On FAU and H-FAU the adsorption complex of $\text{Fe}(\text{CO})_5$ shows broad but well structured bands. On Cs-FAU and FAU* a decreased number of vibrations with

smaller bandwidths is observed. For MAZ and LTL an intermediate picture is typical. In the case of the FAU* sample, the absorption is very similar to that observed in the gas phase, with the strongest bands at 2034 and 2014 cm^{-1} . These spectra reflect differences in the interaction between the iron pentacarbonyl and the zeolite matrix. In particular, when previous considerations of the literature data are taken into account, the i.r. half-bandwidth of the sorption complex and the intensity of the ν_1 vibration around 2120 cm^{-1} can be used as a measure of the strength of the interaction

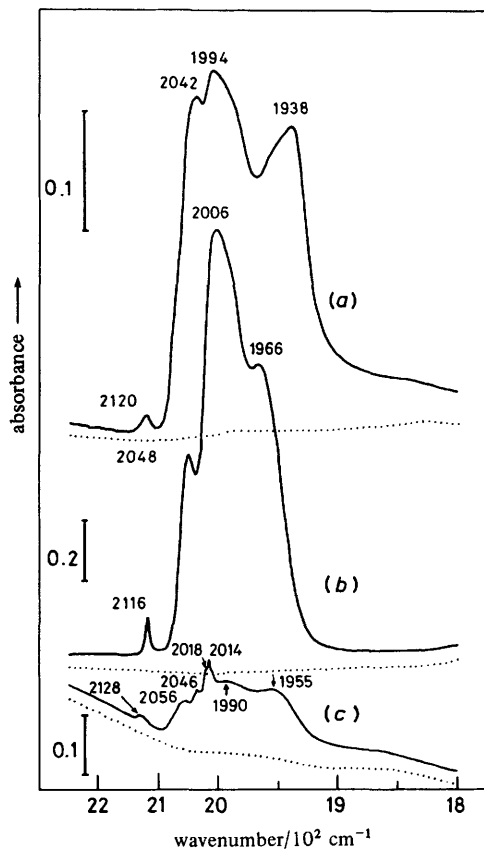


Fig. 5. Infrared spectra of $\text{Fe}(\text{CO})_5$ /zeolite adducts in the CO stretching region at 293 K: (a) $\text{Fe}(\text{CO})_5$ /MAZ saturated; (b) $\text{Fe}(\text{CO})_5$ /LTL saturated for 20%; (c) $\text{Fe}(\text{CO})_5$ /MOR saturated; dotted lines, zeolite wafers degassed at 720 K for 2 h prior to adsorption.

between the zeolite and its adduct. The frequencies of the bands of the pentacarbonyl/zeolite adducts are given in table 5, together with a tentative assignment.

The assignment of the 2120 cm^{-1} band to the ν_1 Raman mode in the $\text{Fe}(\text{CO})_5$ /zeolite adducts requires that, as a result of strong adsorption and specific packing of the pentacarbonyl in the zeolite pores or cages, its original symmetry (D_{3h}) is lowered at least to C_{3v} . This is in line with results from a ^{13}C -n.m.r. line-width broadening study¹³ in which the carbonyl molecule in the $\text{Fe}(\text{CO})_5$ /HY adduct was found to have restricted mobility. It is therefore our conclusion that the i.r. spectrum of $\text{Fe}(\text{CO})_5$ in interaction with the zeolite at room temperature can be explained on the basis of lowered symmetry. In the present work there is no evidence for the formation of

—Fe(CO)₄ species. However, the bands between 1960 and 1938 cm⁻¹ which are assigned to ¹³CO have rather high intensities (table 5). Therefore their assignment to Fe(CO)₄ cannot be excluded unambiguously. The existence of the latter species was only based on a comparison in frequency of *some* bands in the adduct spectrum (2040, 1970 and 1940 cm⁻¹) with the solution spectrum of complexes such as Fe(CO)₄P(CH₃)₃^{11, 12} and does not constitute an unambiguous assignment.

Table 5. I.r. frequencies of Fe(CO)₅/zeolite adducts

proposed assignment	FAU	Cs-FAU	H-FAU	H-FAU ^a	FAU*	MAZ	LTL	MOR
ν_1	2122 w 2060 s	2128/16 w	2120 w	2112 2040	2114/06 w	2120 w	2116	2128 w 2056 s
ν_2	2044 s	2040 sh	2050 s	2030	2033 sh			2046 s
ν_6	2012 s	2012 sh	2020 s	2010	2024 s	2042 s	2048 s	2014 s
ν_{10}	1985 s 1960 sh	1983 s	1986 s 1956 s	1985 1950	2004 s	1994 s	2006 s 1966 s	1990 sh 1955 s
¹³ C	1945 s	1948 sh				1938 s		

^a Ref. (11): this species is assigned by analogy with the frequency of the bands at 2040, 1970 and 1940 cm⁻¹ assigned to —Fe(CO)₄.

Moreover, since no i.r. bands could be detected in the CO bridging range (*i.e.* between 1900 and 1650 cm⁻¹) of the adsorbed carbonyl, at ambient temperature no chemical reaction seems to occur when Fe(CO)₅ is adsorbed on the zeolites. Also no free or physisorbed CO could be detected since the rotation-vibration spectrum around 2153 cm⁻¹ was never observed in the experimental conditions mentioned. The latter bands only become visible when the adduct is heated in a closed system.²⁵

Since the assignment of lower-frequency bands cannot be entirely excluded, and since the extinction coefficient for gaseous or physically adsorbed CO is quite small, the reaction



may occur to some extent without CO being detected. * Carbon monoxide chemisorbed on metallic iron particles exhibits adsorption bands at 2020, 1980 and 1887 cm⁻¹.^{26, 27} Therefore, the appearance of the 2120 cm⁻¹ vibration also cannot be related to decomposition of adsorbed Fe(CO)₅ molecules.

ZEOLITE-ADDUCT INTERACTION DERIVED FROM I.R. INTENSITIES AND HALF-BANDWIDTHS OF SORBED Fe(CO)₅

The half-bandwidth of the absorption complex of Fe(CO)₅ in the frequency range 2100–1900 cm⁻¹ is very much dependent upon the type of zeolite and the nature of the charge-compensating cations (table 6). As explained earlier, for larger values of the half-bandwidth a higher perturbation of the site symmetry is expected, resulting in a stronger interaction between the adduct and the zeolite matrix. In the case of the adduct to H-FAU, a relatively weak hydrogen bond is formed with the supercage hydroxyl groups,²⁵ since the 3645 cm⁻¹ OH bands upon interaction with Fe(CO)₅ shift to *ca.* 3550 cm⁻¹.^{12, 25} At saturation, this process occurs in a quantitative way, since the 3645 cm⁻¹ band disappears completely.

* We are grateful to a referee for pointing out this alternative possibility.

The strength of the interaction between adduct and zeolite is mainly dependent on the nature of the charge-compensation cation. For the FAU structures, the half-bandwidth is higher for the Na-form than for the Cs- and cation-free-forms. For the monodimensional pore systems, the interaction of the adduct with the zeolite seems to be lower in case of the K⁺-form (LTL) in comparison with the Na⁺-form (MAZ).

The zeolite-adduct interaction can be quantified using the intensity ratio between the ν_1 peak and the most intense vibration in the 2100–1900 cm⁻¹ range (table 6). In the case of a gas-phase spectrum this ratio should be zero, indicating the virtual absence of any interactions. At this frequency very small overtone vibrations may sometimes appear with a very low intensity. For the various zeolite adducts investigated here the same conclusions result as those derived from the half-bandwidth measurements.

Table 6. Changes in intensities and half-bandwidths of Fe(CO)₅ in the zeolite adduct

zeolite	half-bandwidth ^a /cm ⁻¹	number of peaks ^b	10 ³ A(ν_1) /A(ν_{\max}) ^c
FAU	135	5	91
H-FAU	115	4	60
Cs-FAU	75	1	24
FAU*	45	2	7
LTL	75	3	87
MAZ	135	3	50
gas phase	—	—	< 3

^a Half-bandwidth of the CO absorption in the 2100–1930 cm⁻¹ range; ^b number of peaks observable in the CO stretching region (2100–1930 cm⁻¹) (ν_1 excluded); ^c ratio of absorbances of ν_1 (around 2120 cm⁻¹) to the maximum absorbance in the 2100–1930 cm⁻¹ region.

CONCLUSIONS

The combined use of gravimetric and infrared methods allows one to obtain detailed information on the state of adsorption of Fe(CO)₅ in different zeolites.

In the zeolites FAU, LTL and MAZ typical micropore filling behaviour is observed, which corresponds to the uptake of *ca.* 3 molecules of sorbate per supercage in the case of faujasite and to 1.5 molecules per channel (or unit cell) in the case of zeolites MAZ and LTL. These sorption values can be rationalized in terms of a simple geometric model in which the cages or pores are completely filled. In the MOR structure the elliptical cross-section of the channels is near the kinetic diameter of Fe(CO)₅ since pore-mouth blocking occurs during adsorption. The sorbate is excluded from the pores of silicalite since only monolayer coverage of the external surface is found for this molecular sieve.

Using the literature assignments for the vibration modes of Fe(CO)₅ an assignment for the i.r. bands observed in the 2200–1900 cm⁻¹ wavenumber range for molecules sorbed on the zeolite is proposed. Most striking is that the ν_1 totally symmetric Raman vibration mode around 2120 cm⁻¹ becomes i.r. active for zeolite-encaged molecules. This suggests that as a result of a strong zeolite-adduct interaction the site symmetry is lowered. The same type of information can be obtained from the half-bandwidth of the CO sorption complex in the 2100–1900 cm⁻¹ wavenumber range.

The nature of this interaction seems to be determined mainly by the nature of the

charge-compensating cations rather than by the geometry and structure of the pores. The zeolite-adduct interaction seems to be stronger for the smaller cations. Surface OH groups form a hydrogen-bond type interaction with the sorbate.

T.B. acknowledges grants from the 'Deutscher Akademischer Austauschdienst', from the Belgian Ministry for Education (Ministerie van Nationale Opvoeding en Nederlandse Cultuur) and the 'Alfried Krupp von Bohlen und Halbach-Stiftung'.

P.A.J. acknowledges a permanent research position as Senior Research Associate from N.F.W.O.-F.N.R.S. (Belgium).

Discussions with Dr F. Schmidt and Prof. W. Gunsser (University of Hamburg) are much appreciated.

- ¹ Y.-Y. Huang and J. R. Anderson, *J. Catal.*, 1975, **40**, 143.
- ² F. Schmidt, W. Gunsser and J. Adolph, *A.C.S. Symp. Ser.*, 1977, **40**, 291.
- ³ W. Gunsser, J. Adolph and F. Schmidt, *J. Magn. Magn. Mater.*, 1980, **15-18(II)**, 1115.
- ⁴ J. B. Lee, *J. Catal.*, 1980, **68**, 27.
- ⁵ D. C. Bailey and S. H. Langer, *Chem. Rev.*, 1981, **81**, 109.
- ⁶ A. Terenin and L. M. Roev, *Spectrochim. Acta*, 1959, **15**, 946.
- ⁷ A. Brenner, *J. Chem. Soc., Chem. Commun.*, 1979, 251.
- ⁸ A. Brenner and D. A. Hucul, *Inorg. Chem.*, 1979, **18**, 2836.
- ⁹ E. Guglielminotti, A. Zecchina, F. Boccuzzi and E. Borello, in *Growth and Properties of Metal Clusters*, ed. J. Bourdon (Elsevier, Amsterdam, 1980), p. 165.
- ¹⁰ J. Phillips, B. Clausen and J. A. Dumesic, *J. Phys. Chem.*, 1980, **84**, 1814.
- ¹¹ D. Ballivet-Tkatchenko, G. Coudurier, H. Mozzanega and I. Tkatchenko, in *Fundamental Research in Homogeneous Catalysis*, ed. M. Tsutsui (Plenum Press, New York, 1979), vol. 3, p. 257.
- ¹² D. Ballivet-Tkatchenko and G. Coudurier, *Inorg. Chem.*, 1979, **18**, 558.
- ¹³ J. B. Nagy, M. van Eenoo and E. G. Derouane, *J. Catal.*, 1979, **58**, 230.
- ¹⁴ J. B. Nagy, M. van Eenoo, E. G. Derouane and J. C. Vadrine, *Magnetic Resonance in Colloid and Interface Science*, ed. J. P. Fraissaid and H. A. Resing (D. Reidel, Dordrecht, 1980), (Nato Adv. Study Inst., Ser. C, vol. 61), p. 591.
- ¹⁵ R. Cataliotti, A. Foffani and L. Marchetti, *Inorg. Chem.*, 1971, **10**, 1594.
- ¹⁶ M. Poliakoff and J. J. Turner, *J. Chem. Soc., Dalton Trans.*, 1973, 1351.
- ¹⁷ D. H. Olson and W. H. Meier, *Atlas of Zeolite Structure Types* (I.Z.A., Polycrystal Book Service, Pittsburg, 1978).
- ¹⁸ C. V. McDaniel and P. K. Maher, *Molecular Sieves* (Society of Chemical Industry, London, 1968), p. 186.
- ¹⁹ H. K. Beyer and I. Belenykaja, in *Catalysis by Zeolites*, ed. B. Imelik, C. Naccache, Y. Ben Taarit, G. Coudurier and H. Praliaud (Elsevier, Amsterdam, 1980), p. 203.
- ²⁰ P. A. Jacobs, H. K. Beyer and J. Valyon, *Zeolites*, 1981, **1**, 161.
- ²¹ M. M. Dubinin, *Prog. Surf. Membr. Sci.*, 1975, **9**, 1.
- ²² Th. Bein and P. A. Jacobs, Part 2 of this series, in preparation.
- ²³ W. F. Edgell, W. E. Wilson and R. Summitt, *Spectrochim. Acta*, 1963, **19**, 863.
- ²⁴ M. Bigorgne, *J. Organomet. Chem.*, 1970, **24**, 211.
- ²⁵ Th. Bein, P. A. Jacobs and F. Schmidt, in *Metal Microstructures in Zeolites*, ed. P. A. Jacobs, P. Jirü, N. Jaeger, G. Schulz-Ekloff (Elsevier, Amsterdam, 1982), p. 111.
- ²⁶ C. J. Pickett and D. Pletcher, *J. Chem. Soc., Dalton Trans.*, 1975, 879.
- ²⁷ G. Blyholder and L. D. Neff, *J. Phys. Chem.*, 1962, **60**, 1464.
- ²⁸ L. H. Jones, R. S. McDowell, M. Goldblatt and B. I. Swanson, *J. Chem. Phys.*, 1972, **57**, 2050.